Combined Action of Variable-Stiffness Devices and Trailing-Edge Flap for Helicopter Hub Loads Reduction

M. Gennaretti, M. Molica Colella, J. Serafini and G. Bernardini

University Roma Tre
Dept. of Mechanical and Industrial Engineering
Via della Vasca Navale 79 - 00146 Rome, Italy

Abstract

The aim of the present paper is the examination of control systems for the alleviation of vibrating loads arising at the rotor hub of helicopters in forward flight. These are obtained by combining the effects of actuated trailing edge flaps with the action of controllable-stiffness devices located at the pitch link and roots of the blades. Control laws are obtained through an optimal control procedure yielding the best compromise between control effectiveness and control effort. The numerical investigation concerns the analysis of performance and robustness of the control techniques examined through application to a four bladed helicopter rotor in level flight. The identification of the most efficient control configuration is also attempted.

List of Symbols

$\mathbf{f}_{aer}$	vector of the generalized aerodynamic forces
$\mathbf{f}_{str}^{nl}$	vector of nonlinear structural contributions
L_v, L_w	dimensionless generalized aerodynamic forces
m	blade mass per unit length
M_ϕ	dimensionless aerodynamic pitching moment
$\mathbf{M}, \mathbf{C}, \mathbf{K}$	mass, damping and stiffness matrices
J	performance index
$\mathbf{q}$	vector of the generalized coordinates
R	rotor radius
T	tension
$\mathbf{T}$	transfer matrix
$\mathbf{u}$	vector of control variables
v, w	displacements of the elastic axis
$\mathbf{W}_u, \mathbf{W}_z$	weighting matrices
x	dimensionless blade span coordinate
$\mathbf{z}$	vector of hub loads harmonics
β	trailing-edge flap deflection
θ	section pitch angle
κ	dimensionless torsion rigidity
Λ_1	dimensionless flap bending stiffnesses
Λ_2	dimensionless lead-lag bending stiffnesses
η	dimensionless mass radii of gyration
ϕ	elastic torsion deflection
Ω	blade angular velocity

1. Introduction

This work deals with the analysis of control systems devoted to the alleviation of helicopter vibratory hub loads. Indeed, rotational and translational motion combined with the $1/rev$ cyclic pitch control, and with the resulting complex aerodynamic environment in which helicopter rotor blades operate (given by wake inflow, dynamic stall and reverse-flow effects) cause blade periodic elastic deformations and transmission of vibratory loads at the hub and hence at the fuselage. In turn, fuselage vibrations affect helicopter performance and reliability and are a critical issue for helicopter designers. They produce acoustic disturbances inside the cabin that may cause unacceptable ride discomfort, and have also a significant impact on the fatigue-life of the structure (and hence on maintenance costs). In addition, vibrations have a negative impact on functionality of instruments located onboard, also making their reading difficult. All this explains why the suppression/alleviation of vibratory hub loads is one of the critical (and most challenging) goals in helicopter design and has received increased attention by rotorcraft researchers in the last decade (see, for instance, Refs. [1], [2] and [3]).

Here, we examine the reduction of the vibrating hub loads through the combined use of controllable-stiffness devices (for instance, smart springs [4]) and trailing-edge flaps. In particular, the controllable-stiffness devices are assumed to be embedded both at the blade root to modify the bending stiffness and in the pitch link to modify the torsional dynamics of the blade. A sketch of the

blade with inclusion of these control devices is given in Fig. 1. Specifically, the investigation is aimed at the analysis of both effectiveness and robustness of such a kind of control technique, and is accomplished in the framework of the SHARCS project [5]. The laws of the cyclic stiffness variation and flap deflection is obtained by an optimal control process based on the minimization of a cost function which includes hub load and control input harmonics, under the constraint of compatibility with equations governing the blade aeroelasticity.

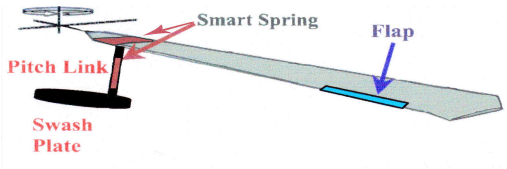

Figure 1. Blade with flap and controllable-stiffness devices

Blade aeroelastic modeling comes from coupling structural dynamics equations with unsteady aerodynamic loads. The blade structural dynamics is described through the nonlinear flap-lag-torsion equations of motion presented by Hodges and Dowell [6]. These are related to a beam-like model and are valid for straight, slender, homogeneous, isotropic, nonuniform, twisted blades undergoing significant deflections. These equations are forced by the aerodynamic loads. Akin to several rotor prediction tools commonly used by helicopter industries, the aerodynamic loads are simulated through 2D, quasi-steady, aerodynamic models including flap effects, with wake-inflow corrections obtained either analytically, or as predicted by a 3D, unsteady, free-wake, BEM computational tool for potential flows [7]. The final aeroelastic equations are solved by applying the Galerkin method for the space discretization, followed by a harmonic balance approach for the time integration [8]. Vibratory hub loads are evaluated by integrating inertial loads and aerodynamic loads along the span of each blade.

The numerical investigation examines effectiveness and robustness of control techniques based on several combinations of the trailing edge flap and the variable stiffness devices, considering the vibrating hub loads arising in a four-bladed rotor in level forward flight. The study will attempt to identify the most efficient control configuration.

2. Model for blade dynamics

The starting point for the identification of blade flap and variable-stiffness devices optimal control actuation is the definition of the aeroelastic model through which the helicopter rotor behavior may be simulated: it is essential both in the control law synthesis process and for the validation of the performance of the control procedure. Here, the aeroelastic equations are obtained by coupling a beam-like rotor blade structural description with the aerodynamic loads from a 2D, quasi-steady model that takes into account wake inflow effects and trailing-edge flap influence.

The blade equations are based on the nonlinear bending-torsion formulation presented by Hodges and Dowell [6], that is valid for straight, slender, homogeneous, isotropic, nonuniform, twisted blades, undergoing moderate displacements. Indeed, second order terms are retained in the equations after the application of an ordering scheme that drops third-order terms (with respect to bending slope) not contributing to damping. For a hub-centered orthogonal coordinate system fixed with the undeformed blade, having spanwise x-axis and the y-axis parallel to the plane of rotation, the lead-lag, $v(x,t)$, and flap, $w(x,t)$, displacements of the blade elastic axis (aligned, respectively, with y and z axes), along with the cross-section rotation, $\phi(x,t)$, about the deformed elastic axis are governed by the following three dimensionless integro-differential equations [6]

$$\begin{aligned}&[(\Lambda_2-\Lambda_{21}\sin^2\theta)v'']''+\Lambda_{21}[\phi w''\cos(2\theta)-\phi v''\sin(2\theta)]''\\&+\frac{\Lambda_{21}}{2}[w''\sin(2\theta)]''-(Tv')'-e_A\,T\,\cos(\theta+\phi)\\&=L_v(v,w,\phi,\beta)+p_y(v,w,\phi,\beta)-q_z'(v,w,\phi,\beta)\end{aligned}\tag{1}$$

$$\begin{aligned}&[(\Lambda_1+\Lambda_{21}\sin^2\theta)w'']''+\Lambda_{21}[\phi v''\cos(2\theta)+\phi w''\sin(2\theta)]''\\&+\frac{\Lambda_{21}}{2}[v''\sin(2\theta)]''-(Tw')'-e_A\,T\,\sin(\theta+\phi)\\&=L_w(v,w,\phi,\beta)+p_z(v,w,\phi,\beta)+q_y'(v,w,\phi,\beta)\end{aligned}\tag{2}$$

$$\begin{aligned}&\Lambda_{21}[(w''^2-v''^2)\sin\theta\cos\theta+v''w''\cos(2\theta)]-\kappa\phi''\\&-[\eta^2K\,T\,(\phi+\theta)']'-e_A\,T\,(w''\cos\theta-v''\sin\theta)\\&+\kappa_{pl}\,\phi\,\delta(x-x_h)=M_\phi(v,w,\phi,\beta)+q_x(v,w,\phi,\beta)\\&+v'q_y(v,w,\phi,\beta)+w'q_z(v,w,\phi,\beta)\end{aligned}\tag{3}$$

where the tension, T, is given by

$$T=\int_x^1 p_x(v,w,\phi)\,\mathrm{d}\bar{x}\tag{4}$$

and $(\,)'$ denotes derivation with respect to dimensionless spanwise coordinate. The blade loading terms due to section inertial forces, p_x, p_y, p_z, section inertial moments, q_x, q_y, q_z, and aerodynamic loads per unit length, L_v, L_w, M_ϕ, are functions of the blade section degrees of freedom. In the equations above, dimensionless lengths are related to the blade radius, R, while dimensionless time coincides with blade azimuth position. The bending equations, Eqs. (1) and (2), have been obtained by division by the parameter $m\Omega^2R$, while the torsion equation, Eq. (3), is the result of division by the parameter $m\Omega^2R^2$, with m denoting the reference blade mass

per unit length and Ω denoting the angular velocity of the blade. Moreover, Λ_1 and Λ_2 are the dimensionless flap and lead-lag bending stiffnesses, respectively, $\Lambda_{21} = \Lambda_2 - \Lambda_1$, κ is the dimensionless torsion rigidity, η is the dimensionless sectional mass radius of gyration, K is the square of the ratio between the blade cross-section polar radius of gyration and the blade cross-section mass radius of gyration, whereas θ is the section pitch angle and e_A is the tensile offset (see [6] for details).

The effects of the control action performed through activation of trailing-edge flaps and variable-stiffness devices located at blades root and pitch link are included in Eqs. (1)-(3). In particular, the angle β denotes the deflection of flaps which affect aerodynamic and inertial loads at those blade sections where they are present; in addition, the effect of the pitch-link variable-stiffness device is simulated as a time-varying torsional spring, κ_{pl}, at the pitch hinge location, x_h, [see Eq. (3)], whereas the embedded smart springs devoted to changing bending stiffnesses are located in the blade root region, $x_i < x < x_e$, and their effects are simulated assuming that $\Lambda_1 = \Lambda_1^0 + \Delta\Lambda_1[H(x-x_i) - H(x-x_e)]$ and $\Lambda_2 = \Lambda_2^0 + \Delta\Lambda_2[H(x-x_i) - H(x-x_e)]$, with $\Delta\Lambda_1$ and $\Delta\Lambda_2$ denoting the bending stiffnesses time variations.

Akin to several rotor prediction tools commonly used by helicopter industries, the aerodynamic loads on the blade are analyzed by using a two-dimensional, quasi-steady model with wake-inflow corrections (mainly, to take into account the 3D effects due to the complex trailing vortices structure released by the rotor blades). It is based on the Theodorsen [9] and Greenberg [10] theories, under the assumption of very low frequency analysis, for which the lift deficiency function is constant and equal to one (see [12] for details). The wake-inflow on the rotor disk is obtained either analytically [11], or numerically by a 3D, unsteady, free-wake, BEM computational tool for potential flows [7].

Combining Eqs. (1)-(3) with the aerodynamic loads yields the rotor aeroelastic model to be solved. The space discretization of the equations is performed through the Galerkin method, based on elastic deformations described as a linear combination of suitable linearly independent shape functions that satisfy the geometric homogeneous boundary conditions corresponding to the structure constraints (for instance, for a hingeless blade they are chosen as bending natural modes of a cantilever beam). The resulting aeroelastic system consists of a set of nonlinear ordinary differential equations of the type

$$\mathbf{M}(t)\,\ddot{\mathbf{q}} + \mathbf{C}(t)\,\dot{\mathbf{q}} + \mathbf{K}(t)\,\mathbf{q} = \mathbf{f}_{str}^{nl}(t,\mathbf{q}) + \mathbf{f}_{aer}(t,\mathbf{q}) \quad (5)$$

where $\mathbf{q}$ denotes the vector of the Lagrangean coordinates of blade, whereas $\mathbf{M}, \mathbf{C}$, and $\mathbf{K}$ are time-periodic, mass, damping, and stiffness structural matrices representing the linear structural terms. Nonlinear structural contributions are collected in $\mathbf{f}_{str}^{nl}$, whereas the generalized aerodynamic forces are collected in $\mathbf{f}_{aer}$. Note that the control variables, $\beta, \Delta\Lambda_1, \Delta\Lambda_2$ and κ_{pl}, mainly affect generalized aerodynamic forces and stiffness matrix. Finally, Eq. (5) is integrated through a harmonic balance approach. It consists of: (i) expressing LHS and RHS of Eq. (5) in terms of Fourier series; (ii) equating the resulting coefficients; (iii) solving the corresponding algebraic set of equations in terms of the unknown Fourier coefficients of the Lagrangean coordinates of the problem. Once the steady periodic blade deformations are determined, vibratory hub loads are evaluated by integrating along the span the corresponding inertial and aerodynamic loads and combining the contributions from each rotor blade.

3. Identification of optimal control law

Here, the objective is to identify blade flaps cyclic motion and cyclic pitch link and blade root smart spring stiffness variations such that vibrating hub loads are reduced as much as possible. Following an approach already used in the past by other authors that have faced the problem of helicopter vibration control [1], [2], [3], [13], this is achieved through an optimal procedure that consists of minimizing the following performance index

$$J = \mathbf{z}^{\mathrm{T}}\,\mathbf{W}_z\,\mathbf{z} + \mathbf{u}^{\mathrm{T}}\,\mathbf{W}_u\,\mathbf{u} \quad (6)$$

where $\mathbf{u}$ is the vector collecting the control input amplitudes to be determined (harmonics of flap deflection, pitch link and blade root bending stiffnesses, in our case), $\mathbf{z}$ is the vector of the quantities to be reduced (hub loads harmonics, in this problem), while $\mathbf{W}_z$ and $\mathbf{W}_u$ are weighting matrices that are defined so as to get the best compromise between control effectiveness and control effort. Because of the inherently time-periodic nature of the problem, this control approach involves only the harmonics of input and output variables, without concerning the evolution of transients. In the present problem, for a N-bladed rotor, the output vector consists of the N/rev sine and cosine harmonics of forces and moments at the hub, while the control inputs are the sine and cosine harmonics of flap deflection, β, pitch link stiffness, κ_{pl}, and blade root smart spring stiffnesses, $\Delta\Lambda_1, \Delta\Lambda_2$, that are effective for control.

Akin to the standard optimal LQR control method (of which the present approach may be interpreted as the natural extension for the application to the control of the steady-periodic behavior of a system governed by a nonlinear, periodic-coefficient differential equation), the minimization of the cost function is obtained under the constraint of satisfying the governing equation of the system controlled. Such constraint is not directly represented by Eq. (5), but rather is given by the following linearized relationship (about a reference input state, $\mathbf{u}_{n-1}$) between control inputs, $\mathbf{u}$, and system response, $\mathbf{z}$,

$$\mathbf{z}_n = \mathbf{z}_{n-1} + \mathbf{T}_{n-1}\,(\mathbf{u}_n - \mathbf{u}_{n-1}) \quad (7)$$

where $\mathbf{T}_{n-1}$ is the (Jacobian) transfer matrix that may be obtained numerically from solutions of Eq. (5). Note

that the nonlinear behavior of the rotor aeroelastic response implies that the transfer matrix is not constant, being a function of the reference input state. Then, combining Eq. (6) with Eq. (7) and minimizing the resulting cost function yields the following optimal control input

$$\mathbf{u}_n = \mathbf{G}_u\,\mathbf{u}_{n-1} - \mathbf{G}_z\,\mathbf{z}_{n-1} \tag{8}$$

where the gain matrices are given by

$$\begin{aligned}\mathbf{G}_u &= \mathbf{D}\,\mathbf{T}_{n-1}^{\mathrm{T}}\,\mathbf{W}_z\mathbf{T}_{n-1}\\ \mathbf{G}_z &= \mathbf{D}\,\mathbf{T}_{n-1}^{\mathrm{T}}\,\mathbf{W}_z\end{aligned}$$

with

$$\mathbf{D} = (\mathbf{T}_{n-1}^{\mathrm{T}}\mathbf{W}_z\mathbf{T}_{n-1} + \mathbf{W}_u)^{-1}$$

Equation (8) has to be used in a recursive way: starting from a given control input and corresponding output, the law of the optimal controller is updated until convergence. In a semi-active control process Eq. (8) directly yields the control actuation laws to be applied, otherwise this procedure gives the gain matrices to be implemented in a closed-loop control process in which, at each n-th control step, measured vibrating hub loads and corresponding control inputs are used as a feedback to update the control law. In this case, the time interval between each control step should be long enough to allow the helicopter to reach the steady-periodic state corresponding to the updated control inputs [1].

4. Numerical results

The control approach presented above has been applied to alleviate the vibrating loads arising during level flight conditions at the hub of a Bo-105-like four-bladed main rotor. The radius of this rotor is $R = 4.93$m, the blades have constant chord, $c = 0.395$m, and linear twist angle equal to $-8°$; in addition, bending and torsional nondimensional stiffnesses (as well as cross-section mass radius of gyration and mass per unit length) have been assumed to be uniform along the blade span and, respectively, equal to $\Lambda_1 = 0.008345$, $\Lambda_2 = 0.023198$, $\kappa = 0.00225$ (see [2], for further details). The flight configuration with advance ratio $\mu = 0.3$ has been examined, with trim controls related to blade rotational speed $\Omega = 40$rad/s.

In the first step of the analysis the control matrices, $\mathbf{G}_u$ and $\mathbf{G}_z$, have been identified as those yielding the optimal hub loads reduction, under the limitation of requiring a maximum flap deflection of $\pm 4°$, maximum amplitudes of flap and lead-lag bending stiffness cyclic variations equal to 10% of Λ_1 and Λ_2, respectively, and maximum amplitude of pitch link stiffness variation equivalent to 10% of κ (such constraints are introduced to take into account the operational limitations that would unavoidably arise during the practical implementation of the control). Specifically, considering an aeroelastic rotor model based on the wake inflow given by Drees [11], the optimal weighting matrices and the corresponding control variables cyclic evolution have been determined using a local controller approach, with the transfer matrix in Eq. (7) given by a preliminary analytical approximation based on a least square procedure. Indeed, this approach allows a search of the optimal control law that is as fast as that using a global controller (*i.e.,* considering a constant transfer matrix), and much faster than the local controller ones based on the numerical evaluation of the transfer matrix at each step of the control process. Note that the application of a local controller is needed because of the presence of the trailing edge flap deflection among the control variables: indeed, the elements of the transfer matrix related to the action of the flap are those that more significantly depend on the control variables state about which are evaluated.

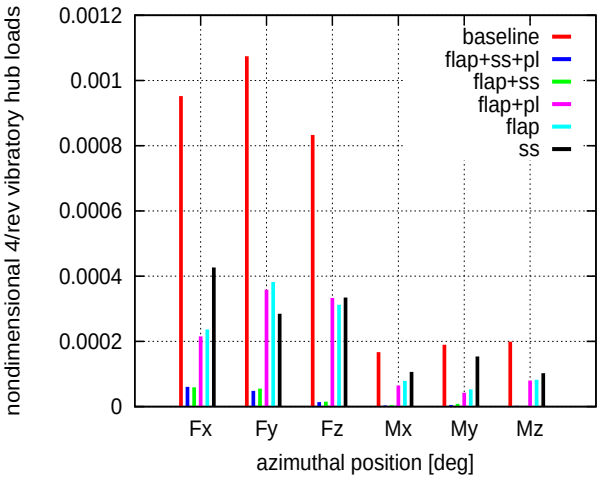

Figure 2. Hub loads, Drees wake inflow

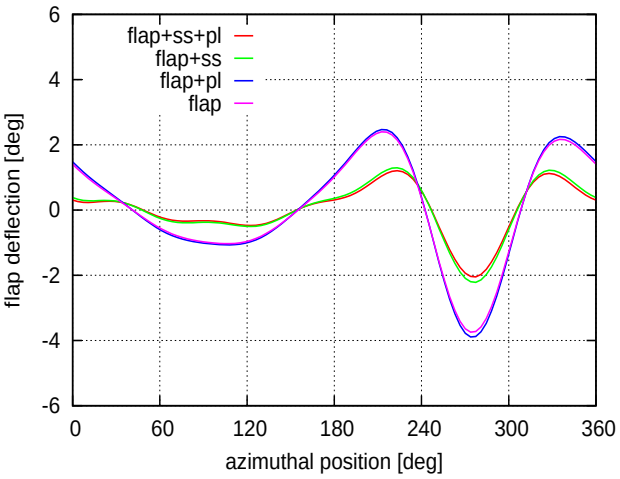

Figure 3. Flap deflections time history

Figure 2 compares the baseline vibrating hub loads (*i.e.,* without any control actuation) with those resulting from the application of control laws identified using several combinations of the control variables considered in this

work. Figure 3 depicts the flap deflection time histories used in the control procedures applied for the results in Fig. 2, while Figs. 4, 5 and 6 show the corresponding bending stiffnesses and pitch link stiffness variations during one blade revolution (in this analysis the $2-5/rev$ control variables harmonics have been included, in that are those most effective for the control of a four-bladed rotor). All the control approaches

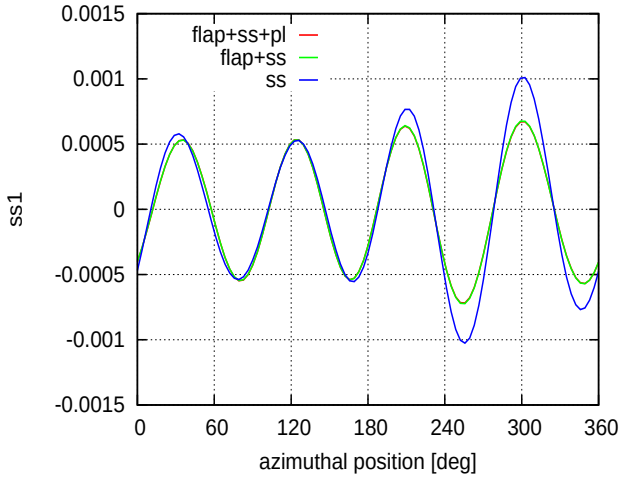

Figure 4. Flap bending stiffness time history

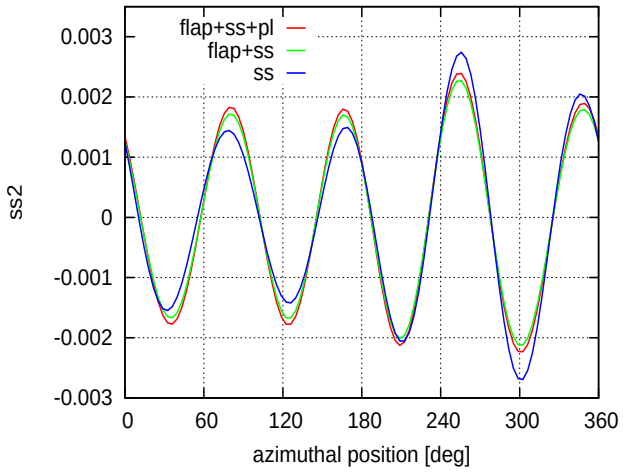

Figure 5. Lag bending stiffness time history

applied seem to yield significant alleviations of the vibrating loads, however the most effective strategies are those in which there is the combined use of cyclic trailing edge flap deflections and blade root stiffness variations through smart springs. In addition, the control laws based on such combinations require lower control variables effort with respect to the other techniques (see Figs. 3-5). The results given by the application of the only pitch link stiffness variation have not been included in that, at least for the stiffness range that has been considered in this work, it does not produce significant vibrations reductions.

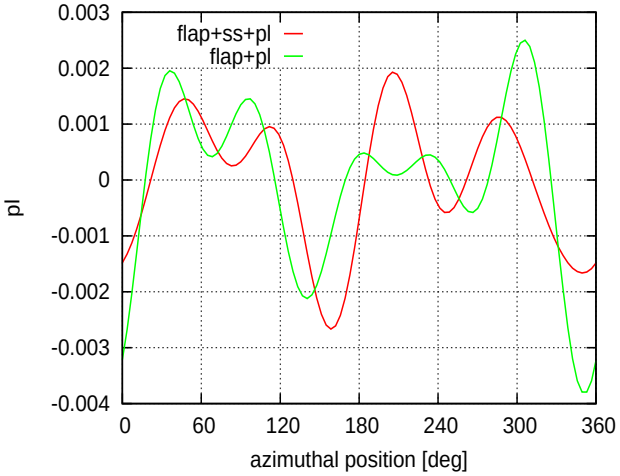

Figure 6. Pitch link stiffness time history

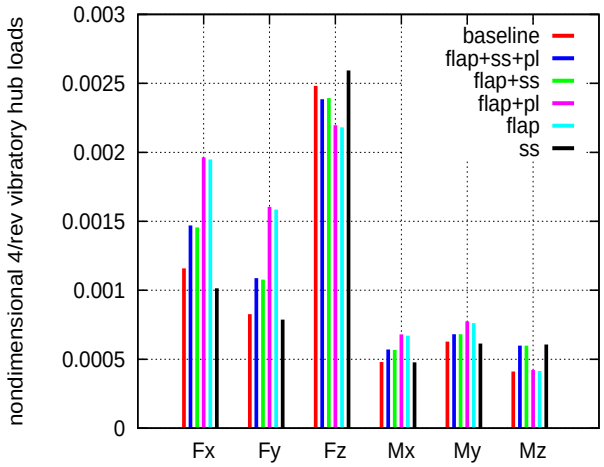

Figure 7. Hub loads without feedback, free-wake inflow

The effectiveness of the control techniques dramatically changes when the cyclic control variables histories are applied to a rotor aeroelastic model that uses a more realistic wake inflow based on a BEM free-wake solver [7]. This is demonstrated by Fig. 7 that shows the inefficiency of the controls which, for some loads, even increase the vibratory level. Indeed, with respect to the model based on the Drees wake inflow, the application of a wake inflow based on a free-wake solver introduces higher frequencies in the aerodynamic loads, and hence significantly modifies the harmonic loads in the rotating frame that participate to the vibrating loads in the hub frame (note that the baseline vibrating hub loads in Fig. 7 are significantly increased with respect to those in Fig. 2). Thus the cyclic controls identified with the simpler aeroelatic model may result inefficient.

The problem of identifying the control laws with numerical simulations that unavoidably differ from the real rotor aeroelastic behavior may be alleviated by using accurate modeling, but not eliminated. Next, we exam-

ine a strategy to overcome this problem that includes a feedback process in the definition of the flap actuation and analyze the benefit of using more accurate simulations in the control identification process. In particular, leaving unchanged the actuation laws regarding the smart springs at blade root and pitch link that have been identified with the simpler aeroelastic model, Eq. (8) is applied recursively to determine the flap deflection that minimize the performance index for the given (feedback) vibrating hub loads (note that if stiffness control variables are also updated in the feedback control process, the procedure does not tends to a converged solution). Figure 8 shows the vibrating hub loads

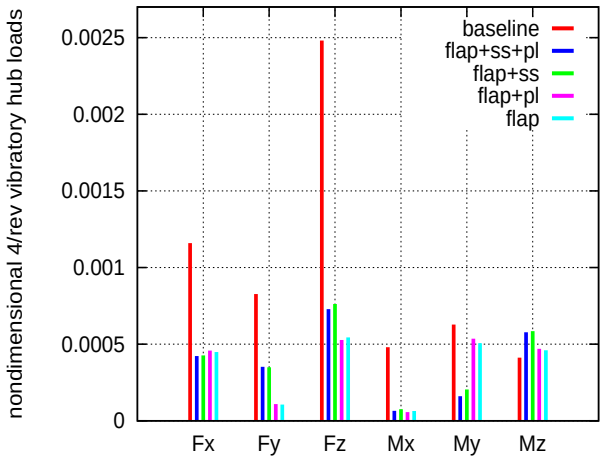

Figure 8. Hub loads with feedback, free-wake inflow

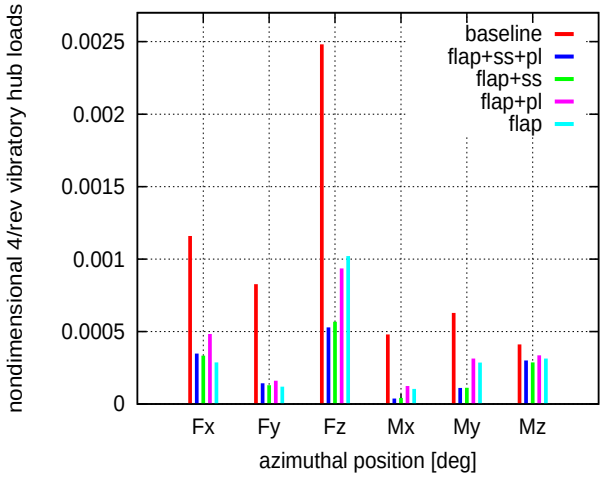

Figure 9. Hub loads with feedback, prescribed-wake synthesis

corresponding to the different control strategies examined here, with the application of the feedback process in the flap actuation law. In this case the results are quite satisfactory, although it is unclear if it is useful to combine flap with root smart spring, rather than controlling with the only trailing edge flap. A clearer answer to such question comes from Fig. 9. It presents the hub loads alleviated using the feedback process for the flap actuation with control matrices $\mathbf{G}_u, \mathbf{G}_z$ in Eq. (8) and the cyclic stiffnesses variations identified with an aeroelastic simulation based on the wake inflow given by a BEM prescribed (undistorted) wake solver. The improved accuracy of the aeroelastic solver applied in the control law identification yields a better performance of the control procedures examined. However, in this case, due to the increased reliability of the cyclic stiffness actuation laws, the combined use of flap and blade root smart spring seems to be the most efficient control procedure (the inclusion of the pitch link stiffness variation seems to have negligible influence). The cyclic flap deflections corresponding to the controlled hub loads in Fig. 9 are depicted in Fig. 10, with their harmonic content given in Fig. 11 which demonstrates the importance of the higher frequency flap motion. Figures 12 and 13 depict the cyclic blade root bending stiffnesses variations that have been identified with the prescribed wake inflow aeroelastic model and have been used to get the hub loads in Fig. 9.

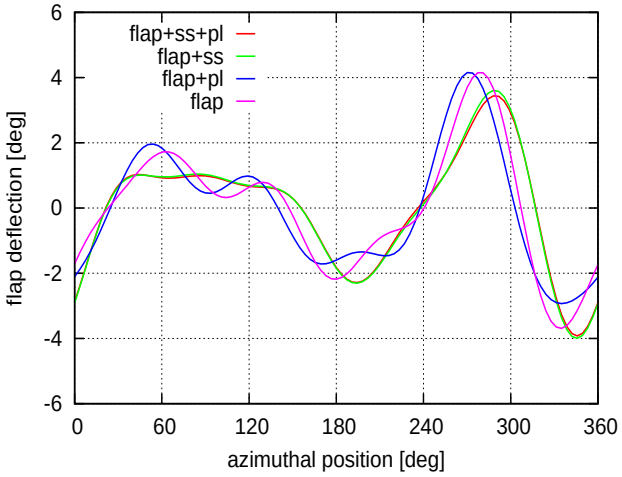

Figure 10. Flap deflections time history

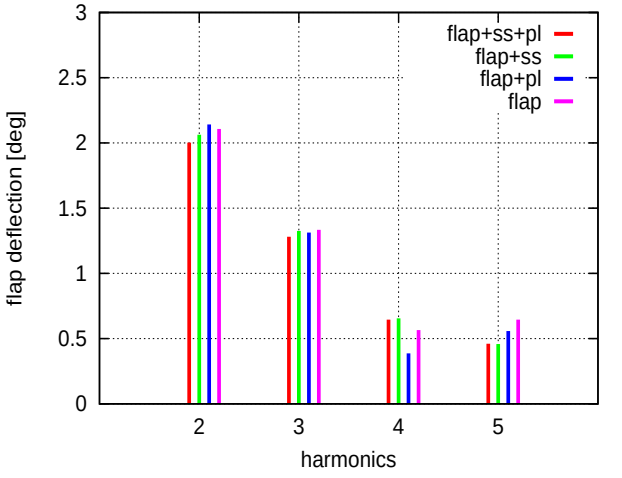

Figure 11. Flap deflections harmonics

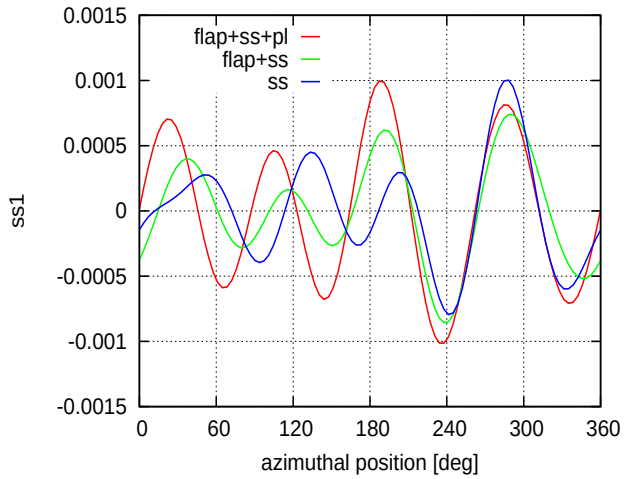

Figure 12. Flap bending stiffness time history

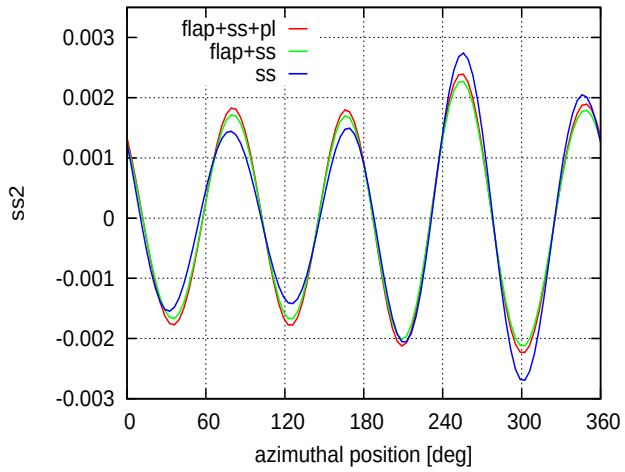

Figure 13. Lag bending stiffness time history

5. Concluding remarks

This work has examined the effectiveness of several optimal control strategies devoted to the alleviation of vibrating loads at helicopter rotor hubs. These strategies have been the results of the combined use of trailing-edge flap and variable stiffness devices at the blade root and pitch link. A particular goal of the work has been the analysis of control performance changes when moving from the control identification rotor model to a more realistic control validation model. Satisfactory load reductions have been obtained during the control law identification process based on the numerical simulations from a rotor aeroelastic tool using a simple wake inflow model. However, the application of the same cyclic actuation laws to a rotor model with a wake inflow predicted from an aerodynamic free-wake solver has produced a totally unsatisfacory load alleviation. In order to get significant load reductions a feedback process has been included in the control procedure. In particular, the control matrices obtained with the simpler model have been applied to update the flap actuation law recursively, from the knowledge of current hub loads, leaving the variable stiffness actuation laws unchanged. Better control performances have been obtained enhancing the accuracy of the aeroelastic identification plant, particularly in terms of the semi-active contribution from the variable stiffness devices. This analysis has shown that the combined use of flap and blade root variable stiffness smart spring is the control strategy yielding the highest level of hub loads alleviations, at least for the control variables oscillation amplitude constraints here considered.

Acknowledgments

This work is part of the research activity developed by University Roma Tre within the project SHARCS coordinated by Prof. F. Nitzsche of Carleton University, Ottawa, Canada.

References

1. Patt, D., Liu, L., and Friedmann, P.P. Rotorcraft Vibration Reduction and Noise Predictions Using a Unified Aeroelastic Response Simulation, *J. of the American Helicopter Society*, 2005, **50**, (1), pp 95-106.
2. Zhang, J. Active-passive hybrid optimization of rotor blades with trailing edge flaps, Ph.D. Dissertation, 2001, Department of Aerospace Engineering, The Pennsylvania State University.
3. Anusonti-Inthra, P. and Gandhi, F. Helicopter vibration reduction through cyclic variations in rotor blade root stiffness, *Journal of Intelligent Material Systems and Structures*, 2000, **11**, (2), pp 153-166.
4. Nitzsche, F., Grewal, A., and Zimcik, D. "Structural Component having Means for Actively Varying its Stiffness to Control Vibrations, U.S. Patent No. 5,973,440, 999. European Patent EP-996570-B1, 2001.
5. Nitzsche, F., Feszty, D., Waechter, D., Pagnano, G., Voutsinas, S., Gennaretti, M., Coppotelli, G., and Ghiringhelli, G.L. The SHARCS Project: Smart Hybrid Active Rotor Control System for Noise and Vibration Attenuation of Helicopter Rotor Blades, 31st European Rotorcraft Forum, Firenze, Italy, 2005.
6. Hodges, D.H. and Dowell, E.H. Nonlinear Equation for the Elastic Bending and Torsion of Twisted Nonuniform Rotor Blades", NASA TN D-7818, 1974.
7. Gennaretti, M. and Bernardini, G. Novel Boundary Integral Formulation for Blade-Vortex Interaction Aerodynamics of Helicopter Rotors, *AIAA Journal*, 2007, **45**, (6), pp 1169-1176.
8. Gennaretti, M. and Bernardini, G. Aeroelastic Response of Helicopter Rotors Using a 3-D Unsteady

Aerodynamic Solver, *The Aeronautical Journal*, 2006, **110**, (1114), pp 793-801.

9. Theodorsen, T. General Theory of Aerodynamic Instability and the Mechanism of Flutter, NACA Report 496, 1935.
10. Greenberg, J.M. Airfoil in Sinusoidal Motion in a Pulsating Stream, NACA TN-1326, 1947.
11. Drees, J.M. A Theory of Airflow Through Rotors and Its Application to Some Helicopter Problems, *Journal of the Helicopter Association of Great Britain*, 1949, **3**, (2), pp 79-104.
12. Gennaretti, M., Molica Colella, M., and Bernardini, G. Alleviation of helicopter vibrating hub loads through cyclic trailing-edge blade flap actuation, ISMA International Conference on Noise and Vibration Engineering, Leuven, Belgium, Sept. 2008.
13. Johnson, W. Self-tuning regulators for multicyclic control of helicopter vibration, NASA TP-1996, 1982.